Cloning and kinetic characterization of *Arabidopsis thaliana* solanesyl diphosphate synthase

Kazutake HIROOKA, Takeshi BAMBA, Ei-ichiro FUKUSAKI and Akio KOBAYASHI[1]

Department of Biotechnology, Graduate School of Engineering, Osaka University, Suita Yamadaoka 2-1, Osaka 565-0871, Japan

trans-Long-chain prenyl diphosphate synthases catalyse the sequential condensation of isopentenyl diphosphate (C_5) units with allylic diphosphate to produce the C_{30}–C_{50} prenyl diphosphates, which are precursors of the side chains of prenylquinones. Based on the relationship between product specificity and the region around the first aspartate-rich motif in *trans*-prenyl diphosphate synthases characterized so far, we have isolated the cDNA for a member of *trans*-long-chain prenyl diphosphate synthases from *Arabidopsis thaliana*. The cDNA was heterologously expressed in *Escherichia coli*, and the recombinant His_6-tagged protein was purified and characterized. Product analysis revealed that the cDNA encodes solanesyl diphosphate (C_{45}) synthase (At-SPS). At-SPS utilized farnesyl diphosphate (FPP; C_{15}) and geranylgeranyl diphosphate (GGPP; C_{20}), but did not accept either the C_5 or the C_{10} allylic diphosphate as a primer substrate. The Michaelis constants for FPP and GGPP were 5.73 μM and 1.61 μM respectively. We also performed an analysis of the side chains of prenylquinones extracted from the *A. thaliana* plant, and showed that its major prenylquinones, i.e. plastoquinone and ubiquinone, contain the C_{45} prenyl moiety. This suggests that At-SPS might be devoted to the biosynthesis of either or both of the prenylquinone side chains. This is the first established *trans*-long-chain prenyl diphosphate synthase from a multicellular organism.

Key words: isoprenoid, nonaprenyl diphosphate, plastoquinone, prenyltransferase, ubiquinone.

INTRODUCTION

The *trans*-long-chain prenyl diphosphate synthases catalyse the consecutive condensation of isopentenyl diphosphate (IPP; C_5) with allylic diphosphate in the *trans*-configuration to yield the C_{30}–C_{50} prenyl diphosphates [1]. These compounds are utilized for the side chains of prenylquinones found in almost all organisms; these side chains serve to anchor the molecule in membranes [2].

In plants, the major prenylquinones are plastoquinone and ubiquinone. Although both prenylquinones share the structural feature of the *trans*-polyprenyl tail attached to a benzoquinone skeleton, their subcellular localization and biochemical roles are distinct [3]. Plastoquinone exists in the thylakoid membrane of chloroplasts, and acts as an electron carrier between Photosystem II and the cytochrome b_6–f complex in the photosynthetic electron transfer reaction [4]. In contrast, ubiquinone exists in the inner membrane of the mitochondrion, and transfers electrons from the NADH dehydrogenase complex to the cytochrome b–c_1 complex in the respiratory chain reaction [5]. In addition to their function in electron transfer, both prenylquinones, in reduced form, are involved in antioxidant activity [6,7].

The lengths of the polyprenyl side chains differ between plastoquinone and ubiquinone, and even among plant species. It is assumed that the chain lengths depend on the product specificity of *trans*-long-chain prenyl diphosphate synthases that yield their precursors (Scheme 1). However, in plants, the enzymes are largely unknown, except for the identification of their enzymic activity [8].

Farnesyl diphosphate (FPP; C_{15}) synthase and geranylgeranyl diphosphate (GGPP; C_{20}) synthase catalyse similar *trans*-type condensations to give the C_{15} and C_{20} products respectively. To date, many genes encoding these short-chain prenyl diphosphate synthases have been isolated from various organisms, including higher plants, and well characterized [9–15]. In addition, the molecular cloning of *trans*-long-chain prenyl diphosphate synthases from two yeasts [16,17] and several prokaryotes [18–21] has been conducted. These enzymes share several functionally conserved regions [1]. In particular, two aspartate-rich motifs are crucial for the binding of two kinds of substrate: allylic diphosphate, which binds to the first aspartate-rich motif (FARM), and IPP, which binds to the second aspartate-rich motif. Furthermore, mutagenic studies [22] and the three-dimensional structure of avian FPP synthase with an allylic substrate analogue [23,24] have revealed the outline of a basic mechanism of product specificity that is applicable to all *trans*-prenyl diphosphate synthases. According to this mechanism, the processes of chain elongation and termination occur as follows. After binding of the diphosphate moiety of the allylic substrate via bivalent metal ions to the aspartate residues of the FARM, the prenyl chain extends into a hydrophobic pocket surrounded by α-helices in the enzyme during the sequential condensation of IPP [23,24]. Chain elongation is terminated precisely at a defined length by the direct interaction of the ω-terminus of the product with bulky residues upstream of the FARM [22,25–28]. In the case of plant FPP synthase, the two aromatic residues at the fifth and fourth positions before the FARM act as a steric hindrance to define the product length as C_{15} [9–12,27]. On the other hand,

Abbreviations used: At-SPS, *Arabidopsis thaliana* solanesyl diphosphate synthase; At-*trans*-PT, *Arabidopsis thaliana trans*-prenyltransferase; DMAPP, dimethylallyl diphosphate; FARM, first aspartate-rich motif; FPP, farnesyl diphosphate; GGPP, geranylgeranyl diphosphate; GPP, geranyl diphosphate; IPP, isopentenyl diphosphate; LC-MS, liquid chromatography–MS; ORF, open reading frame; RACE, rapid amplification of cDNA ends; SPP, solanesyl diphosphate; UTR, untranslated region.

[1] To whom correspondence should be addressed (e-mail Kobayashi@bio.eng.osaka-u.ac.jp).

The nucleotide sequence data reported will appear in DDBJ, EMBL, GenBank® and GSDB Nucleotide Sequence Databases under accession number AB071514.

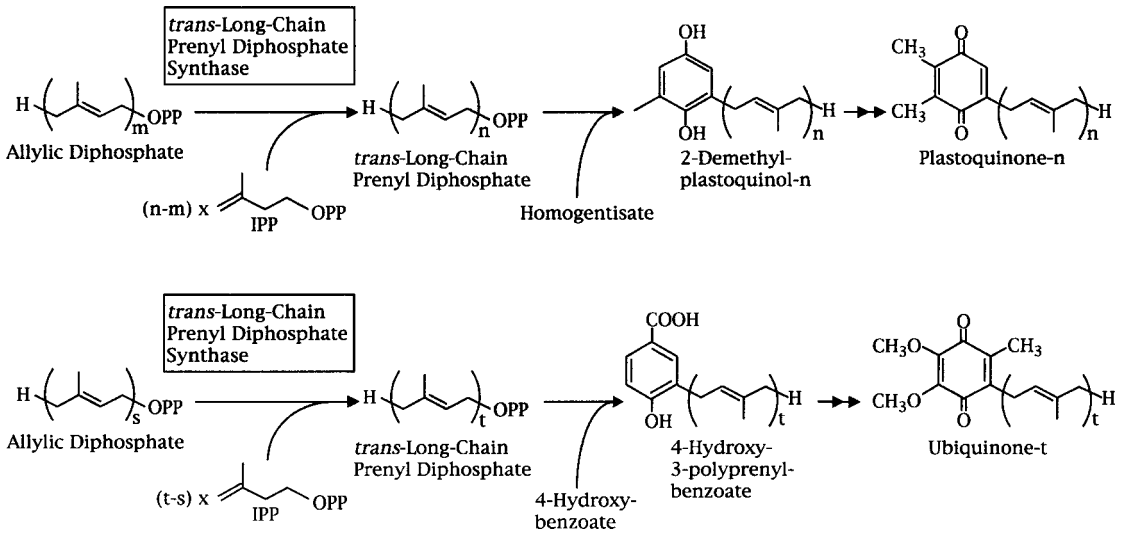

Scheme 1 Two prenylquinone biosynthetic pathways in plants

Each prenylquinone has a hydrophobic tail, which is derived from a *trans*-long-chain prenyl diphosphate synthesized by a specific enzyme. The number of carbons in the isoprene unit differs between plastoquinone and ubiquinone, and among plant species. OPP, diphosphate moiety.

the insertion of two residues within the FARM acts to shorten the product length, independent of the residues preceding the FARM. Plant GGPP synthase has two residue insertions in the FARM (instead of aromatic residues at the fifth and the fourth positions before the FARM) which, consequently, gives the C_{20} product [13–15,27]. In the case of long-chain prenyl diphosphate synthases from micro-organisms, a lack of insertions in the FARM and of aromatic residues immediately before the FARM set the product length to range between C_{30} and C_{50} [21,29,30]. Hence we may expect the region around the FARM of plant long-chain prenyl diphosphate synthases to show the same profile as the enzymes from micro-organisms.

In order to gain more knowledge about the biosynthesis of prenylquinone side chains in plants, we isolated the cDNA encoding *trans*-long-chain prenyl diphosphate synthase from *Arabidopsis thaliana*, based on the information described above, and characterized the recombinant protein.

EXPERIMENTAL

Materials

A. thaliana (ecotype Columbia) seeds were grown on sterile soil at 23 °C with a light intensity of 50 μmol · m^{-2} · s^{-1} and a day length of 16 h. *Escherichia coli* TOP10F' and a pCR®2.1 vector (Invitrogen) were used for the TA cloning. *E. coli* BL21(DE3) and a pET-15b vector (Novagen) were used for expression of the recombinant protein. [4-^{14}C]IPP was purchased from NEN™ Life Science Products. Non-labelled IPP, dimethylallyl diphosphate (DMAPP), geranyl diphosphate (GPP), all-*trans*-FPP, all-*trans*-GGPP and acid phosphatase (potato) were from Sigma. A precoated reverse-phase TLC plate (RP-18) was from Merck.

DNA sequencing

Plasmid DNA for sequencing reactions was prepared with the Quantum Prep® Plasmid Miniprep Kit (Bio-Rad). The sequencing reaction was performed with the BigDye™ Terminator Cycle Sequencing FS Ready Reaction Kit (Applied Biosystems) using the M13 forward (−20) primer, the M13 reverse primer or a specifically designed primer. The nucleotide sequences were obtained by capillary electrophoresis on an ABI PRISM™ 310NT Genetic Analyser (Applied Biosystems).

cDNA cloning

Total RNA was isolated from the total tissue of 4-week-old *A. thaliana* plants using the RNeasy® Plant Mini Kit (QIAGEN), and purified using the same kit after digestion with DNase I. First-strand cDNA was synthesized by reverse transcription using purified total RNA and ReverTra Ace-α-™ reverse transcriptase (TOYOBO), and then treated with RNase H. To isolate the coding sequence of the candidate *A. thaliana trans*-long-chain prenyl diphosphate synthase (accession number NM_106498), PCR was performed using the first-strand cDNA as the template, and the specific primers At-trans-F (5′-ATGTCGGAATATA-GATTTAGGTACGA-3′) and At-trans-R (5′-CTAATCAATT-CTTTCGAGGTTATACAA-3′), which were designed from sequence information on the database. The PCR product was ligated into a pCR®2.1 vector to give a plasmid designated pCR-At-trans-PT. To determine the 5′-untranslated region (UTR) and 3′-UTR of the entire cDNA corresponding to the above-mentioned coding sequence, 5′- and 3′-rapid amplification of cDNA ends (RACE) were conducted. For 5′-RACE, the 5′-Full RACE Core Set (TaKaRa) was used with the *A. thaliana* total RNA as the template and a set of specific primers: At-trans-RT (5′-pAATAACTTCAAGATTCTC-3′) for reverse transcription; At-trans-1st-F (5′-GCGGTGCTAGCTGGAGATTTC-3′) and At-trans-1st-R (5′-CTTGTGCCGAAAAGCTCATGAAC-3′) for the first PCR; and At-trans-2nd-F (5′-CGTCATGGT-ACTTAGCAAATCTC-3′) and At-trans-2nd-R (5′-CATGT-CACTCTCGTCTAACACAT-3′) for the second PCR. For 3′-RACE, the 3′-Full RACE Core Set (TaKaRa) was used with the *A. thaliana* total RNA as the template and a set of specific primers (At-trans-1st-F for the first PCR and At-trans-2nd-F for the second PCR). These sequence data, combined with those of the coding sequence, were compared with the corresponding genome sequence, and it was confirmed that non-specific muta-

genesis had not been introduced during PCR. The sequence of the full-length cDNA is registered in the DDBJ/GenBank/EMBL/GSDB DNA databases under accession no. AB071514. The open reading frame (ORF) of this cDNA was tentatively designated At-*trans*-PT (*A. thaliana trans*-prenyltransferase).

Expression and purification

In order to introduce restriction endonuclease sites at both ends of At-*trans*-PT, PCR was performed with pCR-At-trans-PT as the template and a pair of primers, At-trans-NdeI-F (5′-CATATGATGACGTCATGTCGGAATATAGATTTA-GGTACG-3′) and At-trans-BamHI-R (5′-GGATCCCTAATC-AATTCTTTCGAGGTTATAC-3′); the *Nde*I and *Bam*HI sites respectively are underlined. The PCR product was subcloned into a pCR®2.1 vector and sequenced. The At-*trans*-PT fragment was then excised with *Nde*I and *Bam*HI and ligated into the same sites of a pET-15b vector, yielding the expression plasmid pET-15-At-trans-PT, which encodes an N-terminal in-frame fusion of At-*trans*-PT protein with the His_6 tag. *E. coli* BL21(DE3) was used as a host for the expression of pET-15-At-trans-PT.

Transformed cells carrying pET-15-At-trans-PT were grown at 37 °C in 1.8 litres of a Luria–Bertani medium supplemented with 60 μg/ml ampicillin until A_{600} reached 1.0. Subsequently, isopropyl β-D-thiogalactopyranoside was added to a final concentration of 1 mM, followed by further cultivation for 3 h at 30 °C. Cells were harvested by centrifugation (4000 ***g***, 10 min) and then disrupted by the addition of BugBuster™ HT (Novagen) supplemented with 1 mM PMSF. All subsequent operations were carried out at 4 °C. After centrifugation (8000 ***g***, 30 min) and filtration (0.45 μm), the supernatant was applied to a HiTrap Chelating HP column (Amersham Biosciences) charged with Ni^{2+} and equilibrated with buffer 1 (20 mM sodium phosphate, 0.5 M NaCl, pH 7.4) containing 10 mM imidazole. The column was washed with buffer 1 containing 50 mM imidazole, and eluted with a stepwise gradient of 100–500 mM imidazole in buffer 1. The fractions of the At-*trans*-PT protein were subjected to gel filtration performed on a Superdex 200 HR 10/30 column (Amersham Biosciences) at 0.3 ml/min with buffer 2 (50 mM Mops, 150 mM NaCl, pH 8.0).

After purification, the homogeneity of the At-*trans*-PT protein was confirmed by SDS/PAGE with Coomassie Brilliant Blue staining [31]. Protein concentrations were measured by the method of Bradford with BSA [32] as a standard.

Measurement of enzymic activity and product analysis

Enzymic activity was measured by determination of the amount of [4-^{14}C]IPP incorporated into butanol-extractable polyprenyl diphosphates. The standard assay mixture contained, in a total volume of 200 μl, 100 mM Mops buffer (pH 8.0), 8 mM $MgCl_2$, 0.05 % (w/v) Triton X-100, 50 μM [4-^{14}C]IPP (37 GBq · mol^{-1}), 50 μM allylic substrate (DMAPP, GPP, FPP or GGPP) and 40–50 ng of the purified enzyme. The incubation was carried out at 30 °C for 10 min, and stopped by adding 200 μl of NaCl-saturated water before 10 % of the substrate had been consumed. We confirmed that the addition of NaCl-saturated water completely terminates this enzymic reaction by carrying out the control experiment (results not shown). The reaction products were then extracted with 1 ml of butan-1-ol saturated with NaCl-saturated water, and the radioactivity in the butan-1-ol extract was measured in the d.p.m. mode with an LS 6500 Multi-Purpose Scintillation Counter (Beckman Coulter) and Scintisol® 500 scintillation cocktail (Dojindo).

For kinetic studies, the concentration of the allylic substrate (FPP/GGPP) or of [4-^{14}C]IPP was varied, while the counter-substrate ([4-^{14}C]IPP or FPP/GGPP respectively) was kept at saturating concentration. Kinetic parameters and their standard errors were estimated by non-linear regression analysis using EnzymeKinetics software version 1.5 (Trinity Software).

To analyse the radioactive reaction products, the extracted prenyl diphosphates were hydrolysed to the corresponding alcohols with potato acid phosphatase according to the method reported previously [33]. It was verified that prenyl diphosphates shorter than C_{50} can be hydrolysed completely, and prenyl diphosphates longer than C_{45} can be hydrolysed to some degree, to the corresponding alcohols by this method [29,33]. The alcohols were extracted with n-pentane and analysed by TLC on a reverse-phase RP-18 plate with a solvent system of acetone/water (19:1, v/v). The positions of authentic standards were visualized with iodine vapour, and the absolute radioactivities of the spots were detected with a Bio-image Analyser BAS2000 (Fuji). The product distributions were determined on the basis of the molar ratios of the products that were obtained by division of the absolute radioactivity of each spot by the number of the IPPs incorporated into the corresponding prenyl alcohol.

Analysis of plant prenylquinones

Samples of 10 g (wet weight) of the above-ground parts of 4-week-old *A. thaliana* plants were frozen in liquid nitrogen and ground in a blender. Lipid components including prenylquinones were extracted from the homogenate by reflux of chloroform/methanol (2:1, v/v) for 3 h. The extract was evaporated to dryness, dissolved in n-hexane, and then loaded into a silica gel SepPak column (Waters). The column was washed with n-hexane, followed by elution with n-hexane/diethyl ether (4:1, v/v). The eluate was concentrated and then subjected to HPLC (Shimadzu; LC-10 series) equipped with a photodiode array detector (YMC-Pack ODS-A column; 5 μm; 4.6 mm × 250 mm) at a flow rate of 1.0 ml/min (temperature 40 °C). After injection on to the column equilibrated with 100 % solvent A (methanol/water, 9:1, v/v), the column was eluted with a linear gradient from 0 % to 100 % solvent B (methanol/propan-2-ol, 4:1, v/v) in 40 min, followed by isocratic elution with 100 % solvent B for 20 min. Oxidized forms of plastoquinone and ubiquinone were identified by their absorption spectra, with a λ_{max} of 256 nm (plastoquinone) and 275 nm (ubiquinone). Their reduced forms were detected by their absorption spectra at λ_{max} = 290 nm [34]. To determine the molecular mass of each prenylquinone, we performed liquid chromatography–MS (LC-MS) using a QP8000 LC-MS system (Shimadzu) equipped with an electrospray ionization source [Mightysil column (Kanto Chemical); 5 μm; 2.0 mm × 250 mm] at a flow rate of 0.2 ml/min. After injection on to a column equilibrated with 100 % solvent A′ (solvent A containing 0.1 % formate), the column was eluted by a linear gradient from 0 % to 100 % solvent B′ (solvent B containing 0.1 % formate) in 45 min, followed by isocratic elution with 100 % solvent B′ for 35 min.

RESULTS

Searching the *A. thaliana* database for *trans*-long-chain prenyl diphosphate synthase

Although the mechanism for the determination of product length was identified for *trans*-prenyl diphosphate synthases of archaeal, bacterial and animal origin, we assumed that the same mechanism should hold for plant enzymes producing *trans*-long-chain (C_{30}–C_{50}) prenyl diphosphates [21–30]. Therefore it is likely that these plant enzymes have non-aromatic residues at the fifth and fourth positions before the FARM, and contain no insertions in

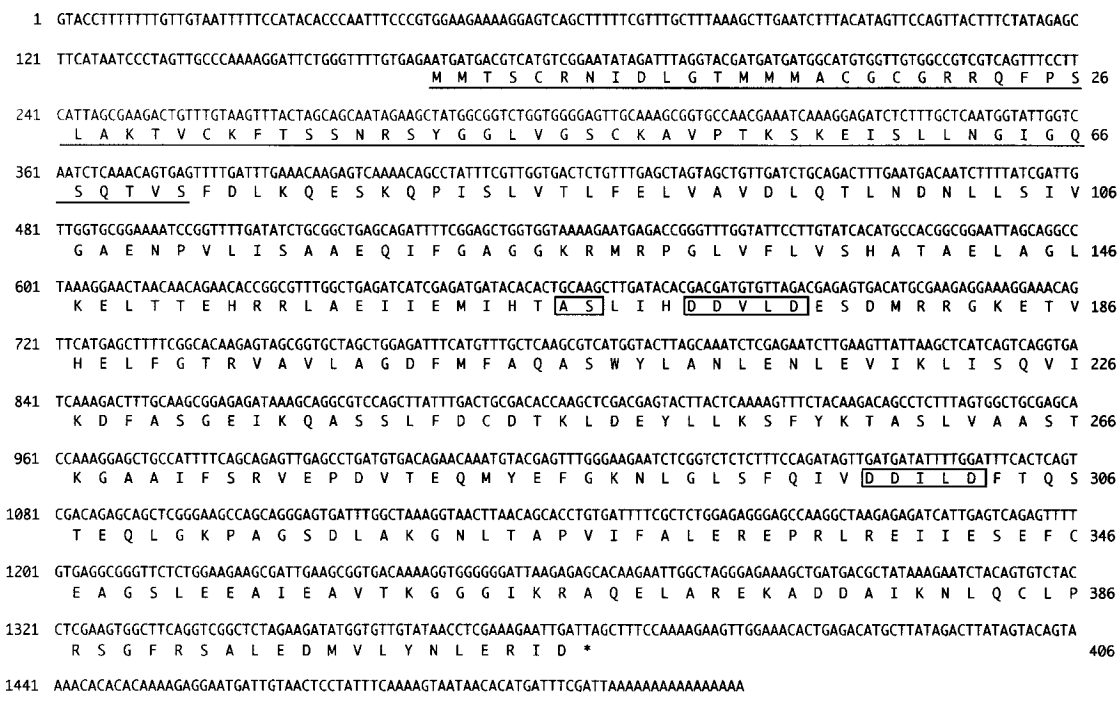

Figure 1 Nucleotide and deduced amino acid sequences of the candidate *trans*-long-chain prenyl diphosphate synthase from *A. thaliana*

Numbers on the left refer to nucleotides; those on the right refer to amino acids. Two aspartate-rich motifs for substrate binding and two non-aromatic residues essential for product specificity are boxed. A putative chloroplast transit peptide is underlined.

the FARM [21,29,30]. Moreover, when a phylogenic tree was constructed among various *trans*-prenyl diphosphate synthases, all non-plant *trans*-long-chain prenyl diphosphate synthases were placed nearer to the group of plant GGPP synthases than to that of plant FPP synthases [22]. This implies that *trans*-long-chain prenyl diphosphate synthase is more similar to GGPP synthase than to FPP synthase in plants.

Thus our attempt to isolate a cDNA coding for a plant *trans*-long-chain prenyl diphosphate synthase was carried out as follows. We first searched the *A. thaliana* sequence database for homologues of GGPS1 (accession no. AAA32797) [13], one of the *A. thaliana* GGPP synthases, using the BLAST search program (http://www.ncbi.nlm.nih.gov/BLAST/). The possible sequences were then screened according to the criterion of whether they had no insertions in the FARM. Consequently, an amino acid sequence (accession no. NP_177972) was selected as the candidate for *trans*-long-chain prenyl diphosphate synthase. This sequence seemed to contain an N-terminal chloroplast transit peptide according to the prediction programs of protein sorting signals and localization sites such as ChloroP (http://www.cbs.dtu.dk/services/ChloroP/) [35,36].

Isolation of the cDNA of the candidate *trans*-long-chain prenyl diphosphate synthase

The coding sequence of NP_177972 (accession no. NM_106498) was obtained by PCR with sequence-specific primers, and first-strand cDNA derived from *A. thaliana* total tissue as the template. Subsequently, 5′- and 3′-UTRs were determined by 5′-RACE and 3′-RACE respectively (Figure 1). The previously registered coding sequence of NM_106498 was constructed using computer programs connecting the putative exons on the genome sequence. We found that the first ATG codon of the ORF of the full-length cDNA obtained here precedes that of the calculated coding sequence. The sequence around this first ATG codon is consistent with the Kozak consensus sequence (RNNAUGR). Thus we supposed that the translation starts from this ATG codon, and we tentatively termed the ORF At-*trans*-PT (for *A. thaliana trans*-prenyltransferase). The At-*trans*-PT protein consists of 406 amino acids. Re-execution of the computer programs for intracellular localization predicted that the At-*trans*-PT protein is also transported into the chloroplast. Hydropathy and transmembrane motif analyses of the At-*trans*-PT protein using the SOSUI system indicated that this protein is a soluble protein and does not contain transmembrane helices large enough to span the lipid bilayers (http://sosui.proteome.bio.tuat.ac.jp/sosuiframe0.html) [37].

The At-*trans*-PT protein shows 23–24 % identity with two *A. thaliana* FPP synthases (accession nos. AAF44787 and S71182) [9–11], 32–38 % identity with five *A. thaliana* GGPP synthases (accession nos. AAA32797, AAB67730, BAB02387, AAD12206 and BAA23157) [13,14], and 33–36 % identity with *trans*-long-

Table 1 Allylic substrate specificity of At-SPS

Enzymic reactions were carried out with 50 μM [4-^{14}C]IPP and 50 μM of the indicated allylic substrate at 30 °C for 10 min. Relative activities were determined based on the activity with FPP.

Allylic substrate	Relative activity (%)
DMAPP	0.34
GPP	0.00
FPP	100
GGPP	111

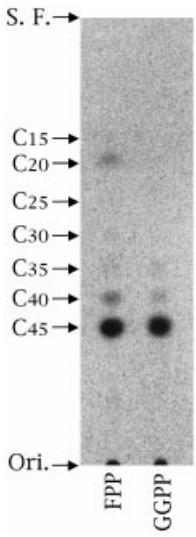

Figure 2 TLC autoradiochromatograms of prenyl alcohols obtained by enzymic hydrolysis of the products formed by At-SPS

The products obtained following incubation of [4-^{14}C]IPP plus FPP (left) or GGPP (right) were analysed by reverse-phase RP-18 TLC, as described in the Experimental section. Ori., origin; S.F., solvent front.

Table 2 Product distribution of At-SPS

Enzymic reactions were carried out with 50 μM [4-^{14}C]IPP plus 50 μM FPP or GGPP at 30 °C for 10 min. The products were then hydrolysed and the resulting alcohols were separated by reverse-phase TLC, as described in the Experimental section. The amount of each prenyl alcohol was determined by dividing the absolute radioactivity by the number of IPPs incorporated into the product.

	Product distribution (%)					
Allylic substrate	C_{20}	C_{25}	C_{30}	C_{35}	C_{40}	C_{45}
FPP	29	5.9	2.9	3.4	6.5	53
GGPP	–	12	0.9	2.2	3.8	82

Table 3 Kinetic parameters of At-SPS

The kinetic parameters of At-SPS were determined at 30 °C for 10 min, as described in the Experimental section. The concentrations of the counter-substrates were set at saturating levels, as indicated. The k_{cat} value was defined by the unit of nmol of IPP converted into products per s by 1 nmol of the dimer enzyme.

Substrate	Counter-substrate	K_m (μM)	k_{cat} (s^{-1})	k_{cat}/K_m ($s^{-1} \cdot \mu M^{-1}$)
FPP	500 μM IPP	5.73 ± 0.45	29.7 ± 0.8	5.19
GGPP	100 μM IPP	1.61 ± 0.21	21.0 ± 1.4	13.1
IPP	20 μM FPP	151 ± 17	14.7 ± 0.7	0.0968
IPP	4 μM GGPP	20.0 ± 1.8	15.0 ± 0.5	0.752

chain prenyl diphosphate synthases derived from four bacteria (accession nos. P19641, P55785, BAA22867 and BAA32241) [18–21] and two yeasts (accession nos. XUBYTP and BAA12314) [16,17]. It is noteworthy that the At-*trans*-PT protein has significant similarity (39 % identity) with *A. thaliana* GPP (C_{10}) synthase (accession no. CAC16849), which catalyses only a single condensation of IPP with DMAPP (C_5) [38].

Functional analysis of the candidate *trans*-long-chain prenyl diphosphate synthase

For functional analysis, the At-*trans*-PT protein was heterologously expressed as a His_6-tagged fusion protein in *E. coli* cells and purified by two chromatographic steps. The M_r of the native At-*trans*-PT protein was estimated to be 108000 by gel filtration chromatography on a Superdex 200 HR column, and the calculated M_r of the single His_6-tagged At-*trans*-PT protein was 46600. Thus the native form of the At-*trans*-PT protein was considered to be dimeric. We performed further investigations using this purified protein.

When the At-*trans*-PT protein was incubated with 50 μM FPP and 50 μM [4-^{14}C]IPP, condensation activity was clearly detected. Maximum activity was achieved under the conditions of pH 8.0 (100 mM Mops buffer), 8 mM $MgCl_2$ and 0.05 % Triton X-100. Additionally, the At-*trans*-PT protein was stable below 40 °C (at pH 8.0 for 10 min).

Four kinds of allylic diphosphates were tested at 50 μM as a primer substrate with 50 μM [4-^{14}C]IPP under the optimum conditions described above. The At-*trans*-PT protein utilized FPP and GGPP as a primer substrate, but not DMAPP or GPP (Table 1). The reaction products with FPP or GGPP were dephosphorylated and then analysed by reverse-phase TLC. When either FPP or GGPP was used as the primer substrate, solanesol (C_{45}) was predominantly detected by TLC analysis, indicating that the At-*trans*-PT protein gave solanesyl diphosphate (SPP; C_{45}) as the major product (Figure 2). Hence we concluded that At-*trans*-PT encodes SPP synthase (EC 2.5.1.11), and we duly designated this ORF as *At-SPS* (*A. thaliana* SPP synthase), and its translated product as At-SPS. When GGPP was used as the allylic substrate, At-SPS produced SPP almost exclusively. In contrast, when FPP was used as the primer substrate, considerable amounts of intermediates, such as GGPP, were formed, although the main product was still SPP (Figure 2 and Table 2). This implies that GGPP should serve as a native primer substrate in *A. thaliana* cells.

The same experiments were conducted with At-SPS from which the His_6 tag had been removed by thrombin cleavage. We confirmed that the specific activity and the product distribution of At-SPS were not affected by the His_6 tag (results not shown). Thus we carried out the kinetic analysis using His_6-tagged At-SPS.

Kinetic analysis of At-SPS

Kinetic constants of At-SPS were determined with [4-^{14}C]IPP and FPP or GGPP as substrates, and the results are summarized in Table 3. At-SPS showed a 3.6-fold lower K_m value for GGPP than that for FPP, and a slightly lower k_{cat} value for GGPP than that for FPP. Consequently the k_{cat}/K_m value for GGPP was 2.5-fold higher than that for FPP, indicating that At-SPS prefers GGPP to FPP as the primer substrate. Moreover, when GGPP was used as the counter-substrate, At-SPS showed a 7.6-fold lower K_m value for IPP than that obtained with FPP as the counter-substrate. Almost equal k_{cat} values for IPP were observed in each case. Consequently the k_{cat}/K_m value for IPP determined with GGPP was 7.8-fold higher than that for IPP with FPP. This result also supports the preference of At-SPS for GGPP over FPP.

Analysis of side chains of prenylquinones from *A. thaliana*

A precise analysis of the lengths of the side chains of plastoquinone and ubiquinone has not been conducted for *A. thaliana*.

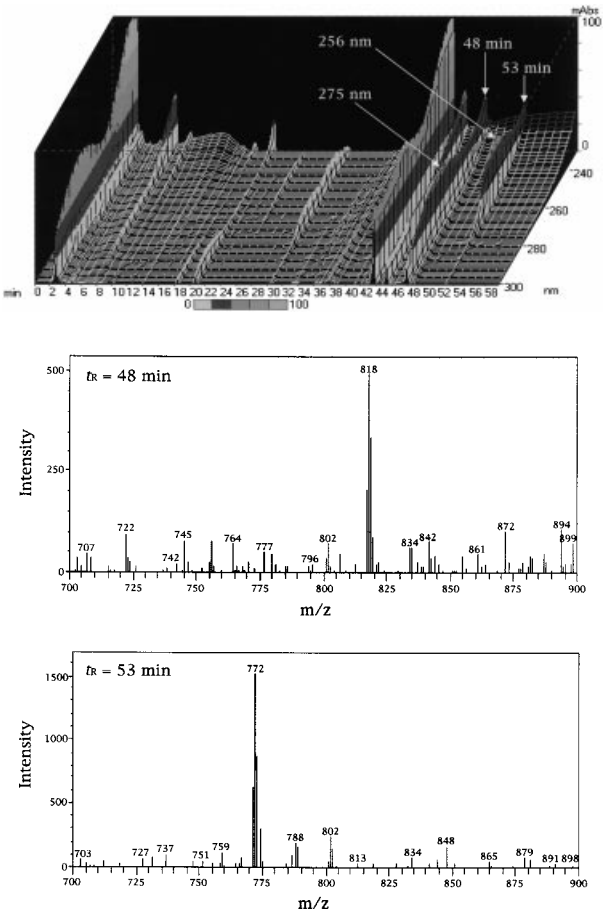

Figure 3 Analysis of *A. thaliana* prenylquinones

Top panel: HPLC chromatogram of *A. thaliana* lipid compounds recorded with a photodiode array detector. A single unimodal peak with a λ_{max} of 275 nm, assignable to oxidized ubiquinone, and a single unimodal peak with a λ_{max} of 256 nm, assignable to oxidized plastoquinone, were observed at retention times of 48 min and 53 min respectively. Bottom panels: mass spectra of the prenylquinones eluted at 48 min and 53 min. These data indicate that the peak at 48 min is ubiquinone-9 [m/z 818 $(M+Na)^+$] and that at 53 min is plastoquinone-9 [m/z 772 $(M+Na)^+$].

To find out which prenylquinone the C_{45} product of At-SPS-catalysed reactions is incorporated into, we analysed the lengths of the side chains of plastoquinone and ubiquinone in the *A. thaliana* plant. Lipid components including prenylquinones were extracted from the above-ground parts of the plant and subjected to HPLC and LC-MS. HPLC analysis showed a single unimodal peak with a λ_{max} of 275 nm assignable to oxidized ubiquinone at 48 min, and a single unimodal peak with a λ_{max} of 256 nm assignable to oxidized plastoquinone at 53 min. Because we did not conduct the extraction procedure under completely anaerobic conditions, almost all of the reduced forms of prenylquinones were oxidized, and consequently no peak with a λ_{max} of 290 nm assignable to the reduced forms was observed (Figure 3, top panel). The oxidized prenylquinones were analysed by LC-MS, and were identified as ubiquinone-9 [$m/z = 818$ $(M+Na)^+$] at 48 min and plastoquinone-9 [$m/z = 772$ $(M+Na)^+$] at 53 min (Figure 3, bottom panels). These analytical results indicate that *A. thaliana* contains only a single molecular species of each ubiquinone and plastoquinone, both of which have the C_{45} prenyl chain, and suggest the possibility that At-SPS is involved in the biosynthesis of either or both of the prenylquinone side chains.

DISCUSSION

In order to gain a better understanding of the biosynthesis of prenylquinone side chains in plants, we have isolated the cDNA for *trans*-long-chain prenyl diphosphate synthase from *A. thaliana* and performed kinetic characterization of the recombinant protein.

The product specificity of the purified recombinant protein revealed that the cDNA encodes a SPP synthase (At-SPS) (Figure 2, Table 2). At-SPS showed maximum activity at pH 8.0, and a substrate preference for GGPP over FPP (Tables 1 and 3). In plant cells, the weakly basic intracellular compartments are the mitochondrial matrix and the chloroplast stroma [3], and it has been reported that GGPP is synthesized mainly in the chloroplastic stroma [14,39]. Moreover, our computer analysis predicted that At-SPS can be transported into chloroplasts. Therefore we speculate that At-SPS is localized in the chloroplast and contributes to plastoquinone biosynthesis, utilizing GGPP for the condensation initiation. This is consistent with a report that the enzymes responsible for the final steps of plastoquinone biosynthesis are localized on the inner envelope membrane of chloroplasts [40]. A kinetic study also showed that At-SPS displays 10–100-fold lower affinity for IPP than for GGPP (Table 3). IPP might be accumulated at high concentrations in the chloroplastic stroma in which At-SPS is localized.

However, our data presented here are not sufficient to conclude that At-SPS is imported into the chloroplast and participates in plastoquinone biosynthesis. Dallner's group [41–43] reported that SPP is synthesized by the condensation of IPP to GPP or GGPP, followed by the transfer of the solanesyl moiety to *p*-hydroxybenzoate and homogentisate to produce the precursors of ubiquinone-9 and plastoquinone-9 respectively in the Golgi/endoplasmic reticulum system of spinach leaves. To clarify the localization of ubiquinone and plastoquinone synthesis in plant cells, it is essential to determine the intracellular localization of At-SPS by methods such as the use of green fluorescent protein fusion proteins or *in vitro* translation followed by incorporation into isolated organelles.

The phylogenetic tree connecting At-SPS and other *trans*-prenyl diphosphate synthases from *A. thaliana* shows that At-SPS is more closely related to GGPP synthases than to FPP synthases, as expected (Figure 4) [44]. Interestingly, At-SPS is also placed phylogenetically as close to GPP synthase as to the GGPP synthases. GPP synthase yields the short-chain product C_{10}, although its region around the FARM is the long-chain type, i.e. with no insertions in the FARM and no aromatic residues before the FARM [22,38]. This exceptional enzyme might regulate its product specificity by an unknown mechanism extraneous to the region around the FARM, and this mechanism might have been lost from At-SPS. GPP synthase is known to be localized in the chloroplast [38] together with GGPS1, the GGPP synthase that is expressed ubiquitously in every tissue and is the most abundant of the five isoenzymes [14]. If At-SPS is also transported into the chloroplast, these enzymes might constitute the subfamily of chloroplastic *trans*-prenyl diphosphate synthases that are evolutionarily related to each other.

Analysis of the side chains of native prenylquinones revealed that *A. thaliana* contains only a single molecular species of each ubiquinone and plastoquinone, with the C_{45} prenyl moiety (Figure 3). The length and nature of the side chains of ubiquinones has been analysed in several plant species. In some

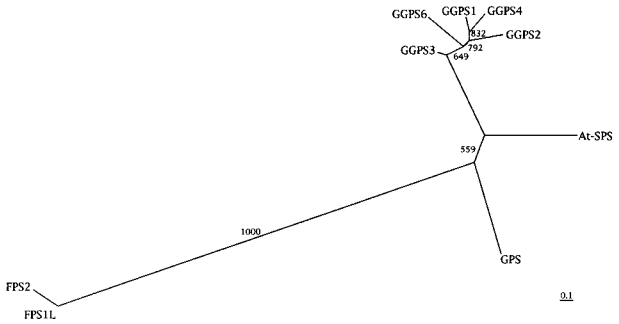

Figure 4 Molecular phylogenetic tree of amino acid sequences of *A. thaliana trans*-prenyl diphosphate synthases

The tree was constructed by the neighbour-joining method [44]. The lengths of the lines indicate the relative distances between nodes. Numbers indicate tree confidence, calculated by bootstrapping (iteration count 1000; maximum value 1000). Enzymes used for alignment are At-SPS (accession no. BAB86941), FPP synthases (FPS1L and FPS2; accession nos. AAF44787 and S71182 respectively), GGPP synthases (GGPS1, GGPS2, GGPS3, GGPS4 and GGPS6; accession nos. AAA32797, AAB67730, BAB02387, AAD12206 and BAA23157 respectively), and GPP synthase (GPS; accession no. CAC16849).

cases, similar ubiquinone spectra have been observed among plant species in the same family. Poaceae and Asteraceae yield ubiquinone-9 predominantly [45–47], and Fabaceae and Solanaceae produce mainly ubiquinone-10 [45,47,48]. However, in the Brassicaceae family, it appears that the major ubiquinone differs among species. *Brassica oleracea* gives mainly ubiquinone-10, with a small amount of ubiquinone-9 [45], whereas *A. thaliana* produces ubiquinone-9 solely, as shown in the present study. The lengths of the ubiquinone side chains in these plants seem to depend on the product specificity of the enzymes that correspond to At-SPS. Thus the At-SPS homologue that yields the C_{50} prenyl diphosphate could be present in plant species in the Brassicaceae family, such as *B. oleracea*. By comparing At-SPS with the At-SPS homologue from *B. oleracea*, the mechanism that defines the product length of C_{45} and C_{50} might be revealed.

The similarity of the product length of At-SPS with the side-chain length of the two prenylquinones from *A. thaliana* implies that At-SPS serves to supply the precursor of the prenyl tail of both prenylquinones. There is some degree of disorder in protein sorting in plant cells, and a given transit peptide might lead to import into both chloroplasts and mitochondria. At-SPS might thus undergo translocation into both organelles. In this case, At-SPS would utilize IPPs derived from different pathways. It has been reported that, in plants, IPP for the plastoquinone prenyl chain is synthesized via a non-mevalonate pathway [49], whereas IPP for the ubiquinone prenyl chain is synthesized via the mevalonate pathway [50].

By screening the *A. thaliana* sequence database using the At-SPS amino acid sequence as a query, we have identified a sequence highly similar to At-SPS (accession no. AAD50025). Judging from the computer programs, this sequence appears to contain a mitochondrial targeting peptide at the N-terminus. Thus this At-SPS homologue might be transported into mitochondria and be involved in the biosynthesis of the ubiquinone side chain. Further detailed analyses of At-SPS and of its homologue may lead to the elucidation of the molecular mechanism of the biosynthesis of prenylquinones in plants.

We are grateful to Dr I. Yanagihara (Osaka Medical Center for Maternal and Child Health, Osaka, Japan) for technical assistance with imaging analysis, and to Dr T. Nakayama (Tohoku University, Japan) for critical reading of the manuscript. This work was performed under a research project of the Development of Transgenic Plants for Production Materials entrusted by the New Energy and Industrial Technology Development Organization (NEDO).

REFERENCES

1 Ogura, K. and Koyama, T. (1998) Enzymatic aspects of isoprenoid chain elongation. Chem. Rev. **98**, 1263–1276
2 Szkopinska, A. (2000) Ubiquinone. Biosynthesis of quinone ring and its isoprenoid side chain. Intracellular localization. Acta Biochim. Pol. **47**, 469–480
3 Hinkle, P. C. and McCarty, R. E. (1978) How cells make ATP. Sci. Am. **238**, 104–123
4 Hope, A. B. (1993) The chloroplast cytochrome *bf* complex: a critical focus on function. Biochim. Biophys. Acta **1143**, 1–22
5 Casey, R. P. (1984) Membrane reconstitution of the energy-conserving enzymes of oxidative phosphorylation. Biochim. Biophys. Acta **768**, 319–347
6 Frei, B., Kim, M. C. and Ames, B. N. (1990) Ubiquinol-10 is an effective lipid-soluble antioxidant at physiological concentrations. Proc. Natl. Acad. Sci. U.S.A. **87**, 4879–4883
7 Hundal, T., Forsmark-Andree, P., Ernster, L. and Andersson, B. (1995) Antioxidant activity of reduced plastoquinone in chloroplast thylakoid membranes. Arch. Biochem. Biophys. **324**, 117–122
8 Sakaihara, T., Honda, A., Tateyama, S. and Sagami, H. (2000) Subcellular fractionation of polyprenyl diphosphate synthase activities responsible for the syntheses of polyprenols and dolichols in spinach leaves. J. Biochem. (Tokyo) **128**, 1073–1078
9 Delourme, D., Lacroute, F. and Karst, F. (1994) Cloning of an *Arabidopsis thaliana* cDNA coding for farnesyl diphosphate synthase by functional complementation in yeast. Plant Mol. Biol. **26**, 1867–1873
10 Cunillera, N., Arro, M., Delourme, D., Karst, F., Boronat, A. and Ferrer, A. (1996) *Arabidopsis thaliana* contains two differentially expressed farnesyl-diphosphate synthase genes. J. Biol. Chem. **271**, 7774–7780
11 Cunillera, N., Boronat, A. and Ferrer, A. (1997) The *Arabidopsis thaliana* FPS1 gene generates a novel mRNA that encodes a mitochondrial farnesyl-diphosphate synthase isoform. J. Biol. Chem. **272**, 15381–15388
12 Gaffe, J., Bru, J. P., Causse, M., Vidal, A., Stamitti-Bert, L., Carde, J. P. and Gallusci, P. (2000) LEFPS1, a tomato farnesyl pyrophosphate gene highly expressed during early fruit development. Plant Physiol. **123**, 1351–1362
13 Scolnik, P. A. and Bartley, G. E. (1994) Nucleotide sequence of an Arabidopsis cDNA for geranylgeranyl pyrophosphate synthase. Plant Physiol. **104**, 1469–1470
14 Okada, K., Saito, T., Nakagawa, T., Kawamukai, M. and Kamiya, Y. (2000) Five geranylgeranyl diphosphate synthases expressed in different organs are localized into three subcellular compartments in Arabidopsis. Plant Physiol. **122**, 1045–1056
15 Hefner, J., Ketchum, R. E. and Croteau, R. (1998) Cloning and functional expression of a cDNA encoding geranylgeranyl diphosphate synthase from *Taxus canadensis* and assessment of the role of this prenyltransferase in cells induced for taxol production. Arch. Biochem. Biophys. **360**, 62–74
16 Ashby, M. N. and Edwards, P. A. (1990) Elucidation of the deficiency in two yeast coenzyme Q mutants. Characterization of the structural gene encoding hexaprenyl pyrophosphate synthetase. J. Biol. Chem. **265**, 13157–13164
17 Suzuki, K., Okada, K., Kamiya, Y., Zhu, X. F., Nakagawa, T., Kawamukai, M. and Matsuda, H. (1997) Analysis of the decaprenyl diphosphate synthase (*dps*) gene in fission yeast suggests a role of ubiquinone as an antioxidant. J. Biochem. (Tokyo) **121**, 496–505
18 Asai, K., Fujisaki, S., Nishimura, Y., Nishino, T., Okada, K., Nakagawa, T., Kawamukai, M. and Matsuda, H. (1994) The identification of *Escherichia coli ispB* (*cel*) gene encoding the octaprenyl diphosphate synthase. Biochem. Biophys. Res. Commun. **202**, 340–345
19 Koike-Takeshita, A., Koyama, T., Obata, S. and Ogura, K. (1995) Molecular cloning and nucleotide sequences of the genes for two essential proteins constituting a novel enzyme system for heptaprenyl diphosphate synthesis. J. Biol. Chem. **270**, 18396–18400
20 Okada, K., Kamiya, Y., Zhu, X., Suzuki, K., Tanaka, K., Nakagawa, T., Matsuda, H. and Kawamukai, M. (1997) Cloning of the *sdsA* gene encoding solanesyl diphosphate synthase from *Rhodobacter capsulatus* and its functional expression in *Escherichia coli* and *Saccharomyces cerevisiae*. J. Bacteriol. **179**, 5992–5998
21 Okada, K., Kainou, T., Tanaka, K., Nakagawa, T., Matsuda, H. and Kawamukai, M. (1998) Molecular cloning and mutational analysis of the *ddsA* gene encoding decaprenyl diphosphate synthase from *Gluconobacter suboxydans*. Eur. J. Biochem. **255**, 52–59
22 Wang, K. and Ohnuma, S. (1999) Chain-length determination mechanism of isoprenyl diphosphate synthases and implications for molecular evolution. Trends Biochem. Sci. **24**, 445–451

23 Tarshis, L. C., Yan, M., Poulter, C. D. and Sacchettini, J. C. (1994) Crystal structure of recombinant farnesyl diphosphate synthase at 2.6 Å resolution. Biochemistry **33**, 10871–10877

24 Tarshis, L. C., Proteau, P. J., Kellogg, B. A., Sacchettini, J. C. and Poulter, C. D. (1996) Regulation of product chain length by isoprenyl diphosphate synthases. Proc. Natl. Acad. Sci. U.S.A. **93**, 15018–15023

25 Ohnuma, S., Hirooka, K., Hemmi, H., Ishida, C., Ohto, C. and Nishino, T. (1996) Conversion of product specificity of archaebacterial geranylgeranyl-diphosphate synthase. Identification of essential amino acid residues for chain length determination of prenyltransferase reaction. J. Biol. Chem. **271**, 18831–18837

26 Ohnuma, S., Narita, K., Nakazawa, T., Ishida, C., Takeuchi, Y., Ohto, C. and Nishino, T. (1996) A role of the amino acid residue located on the fifth position before the first aspartate-rich motif of farnesyl diphosphate synthase on determination of the final product. J. Biol. Chem. **271**, 30748–30754

27 Ohnuma, S., Hirooka, K., Ohto, C. and Nishino, T. (1997) Conversion from archaeal geranylgeranyl diphosphate synthase to farnesyl diphosphate synthase. Two amino acids before the first aspartate-rich motif solely determine eukaryotic farnesyl diphosphate synthase activity. J. Biol. Chem. **272**, 5192–5198

28 Hirooka, K., Kato, T., Matsu-ura, J., Hemmi, H. and Nishino, T. (2000) The role of histidine-114 of *Sulfolobus acidocaldarius* geranylgeranyl diphosphate synthase in chain-length determination. FEBS Lett. **481**, 68–72

29 Ohnuma, S., Hirooka, K., Tsuruoka, N., Yano, M., Ohto, C., Nakane, H. and Nishino, T. (1998) A pathway where polyprenyl diphosphate elongates in prenyltransferase. Insight into a common mechanism of chain length determination of prenyltransferases. J. Biol. Chem. **273**, 26705–26713

30 Hirooka, K., Ohnuma, S., Koike-Takeshita, A., Koyama, T. and Nishino, T. (2000) Mechanism of product chain length determination for heptaprenyl diphosphate synthase from *Bacillus stearothermophilus*. Eur. J. Biochem. **267**, 4520–4528

31 Laemmli, U. K. (1970) Cleavage of structural proteins during the assembly of the head of bacteriophage T4. Nature (London) **227**, 680–685

32 Bradford, M. M. (1976) A rapid and sensitive method for the quantitation of microgram quantities of protein utilizing the principle of protein-dye binding. Anal. Biochem. **72**, 248–254

33 Fujii, H., Koyama, T. and Ogura, K. (1982) Efficient enzymatic hydrolysis of polyprenyl pyrophosphates. Biochim. Biophys. Acta **712**, 716–718

34 Jemiota-Rzeminska, M., Latowski, D. and Strzalka, K. (2001) Incorporation of plastoquinone and ubiquinone into liposome membranes studied by HPLC analysis. The effect of side chain length and redox state of quinone. Chem. Phys. Lipids **110**, 85–94

35 Archer, E. K. and Keegstra, K. (1990) Current views on chloroplast protein import and hypotheses on the origin of the transport mechanism. J. Bioenerg. Biomembr. **22**, 789–810

36 Emanuelsson, O., Nielsen, H. and von Heijne, G. (1999) ChloroP, a neural network-based method for predicting chloroplast transit peptides and their cleavage sites. Protein Sci. **8**, 978–984

37 Hirokawa, T., Boon-Chieng, S. and Mitaku, S. (1998) SOSUI: classification and secondary structure prediction system for membrane proteins. Bioinformatics **14**, 378–379

38 Bouvier, F., Suire, C., d'Harlingue, A., Backhaus, R. A. and Camara, B. (2000) Molecular cloning of geranyl diphosphate synthase and compartmentation of monoterpene synthesis in plant cells. Plant J. **24**, 241–252

39 Bonk, M., Hoffmann, B., Von Lintig, J., Schledz, M., Al-Babili, S., Hobeika, E., Kleinig, H. and Beyer, P. (1997) Chloroplast import of four carotenoid biosynthetic enzymes *in vitro* reveals differential fates prior to membrane binding and oligomeric assembly. Eur. J. Biochem. **247**, 942–950

40 Soll, J., Schultz, G., Joyard, J., Douce, R. and Block, M. A. (1985) Localization and synthesis of prenylquinones in isolated outer and inner envelope membranes from spinach chloroplasts. Arch. Biochem. Biophys. **238**, 290–299

41 Swiezewska, E., Dallner, G., Andersson, B. and Ernster, L. (1993) Biosynthesis of ubiquinone and plastoquinone in the endoplasmic reticulum-Golgi membranes of spinach leaves. J. Biol. Chem. **268**, 1494–1499

42 Osowska-Rogers, S., Swiezewska, E., Andersson, B. and Dallner, G. (1994) The endoplasmic reticulum-Golgi system is a major site of plastoquinone synthesis in spinach leaves. Biochem. Biophys. Res. Commun. **205**, 714–721

43 Wanke, M., Dallner, G. and Swiezewska, E. (2000) Subcellular localization of plastoquinone and ubiquinone synthesis in spinach cells. Biochim. Biophys. Acta **1463**, 188–194

44 Thompson, J. D., Higgins, D. G. and Gibson, T. J. (1994) CLUSTAL W: improving the sensitivity of progressive multiple sequence alignment through sequence weighting, position-specific gap penalties and weight matrix choice. Nucleic Acids Res. **22**, 4673–4680

45 Threlfall, D. R. and Whistance, G. R. (1970) Biosynthesis of ubiquinone–a search for polyprenyl phenol and quinone precursors. Phytochemistry **9**, 355–359

46 Hagimori, M., Matsumoto, T. and Noguchi, M. (1978) Isolation and identification of ubiquinone 9 from cultured cells of safflower (*Carthamus tinctorius* L.). Agric. Biol. Chem. **42**, 499–500

47 Ikeda, M. and Kagei, K. (1979) Ubiquinone content of eight plant species in cell culture. Phytochemistry **18**, 1577–1578

48 Ikeda, T., Matsumoto, T., Kato, K. and Noguchi, M. (1974) Isolation and identification of ubiquinone 10 from cultured cells of tobacco. Agric. Biol. Chem. **38**, 2297–2298

49 Lichtenthaler, H. K., Schwender, J., Disch, A. and Rohmer, M. (1997) Biosynthesis of isoprenoids in higher plant chloroplasts proceeds via a mevalonate-independent pathway. FEBS Lett. **400**, 271–274

50 Disch, A., Hemmerlin, A., Bach, T. J. and Rohmer, M. (1998) Mevalonate-derived isopentenyl diphosphate is the biosynthetic precursor of ubiquinone prenyl side chain in tobacco BY-2 cells. Biochem. J. **331**, 615–621

Received 20 August 2002/12 November 2002; accepted 19 November 2002
Published as BJ Immediate Publication 19 November 2002, DOI 10.1042/BJ20021311